Sustainable Food Technology

ROYAL SOCIETY OF CHEMISTRY

PAPER

View Article Online
View Journal | View Issue

Cite this: *Sustainable Food Technol.*, 2026, **4**, 916

Eco-friendly biofilms from chemically modified Indian teff (*Eragrostis tef*) starch for quality maintenance and shelf-life improvement of green grapes

Ramandeep Kaur Sidhu, * C. S. Riar and Sukhcharn Singh

This study explores the development of sustainable teff starch-based biodegradable films enhanced through oxidation and cross-linking to improve their suitability for food packaging applications. The modified films were evaluated for improved strength, barrier performance, thermal stability, and effectiveness in preserving fresh green grapes. The native film (NF) showed a tensile strength of 3.07 MPa and 38.21% elongation at break. Oxidized films exhibited higher tensile strength, while cross-linked films achieved strengths of 6.62 and 6.71 MPa, maintaining comparable elongation, indicating improved mechanical properties and rigidity. The NF exhibited a water vapor permeability (WVP) of 4.09 $\times$ 10^{-8} g m^{-2} s^{-1} Pa^{-1}. In contrast, oxidized films (2.09 and 2.5 $\times$ 10^{-8} g m^{-2} s^{-1} Pa^{-1}) and cross-linked films (3.00 and 3.98 $\times$ 10^{-8} g m^{-2} s^{-1} Pa^{-1}) showed substantially lower WVP values, reflecting improved moisture barrier properties. The oxidized films and cross-linked films showed increased thermal stability, with decomposition temperatures exceeding 260 °C, highlighting their suitability for durability applications. Oxidized films and cross-linked films demonstrated superior UV protection by significantly increasing UV absorption and reducing harmful transmission, thereby enhancing the preservation of packaged product. Application trials on green grapes revealed that modified films significantly reduced weight loss, preserved firmness, and slowed acidity reduction during storage, extending fruit shelf life. Overall, these findings establish chemically modified teff starch films as promising next-generation biodegradable packaging materials with reinforced strength, stability, and preservation performance—offering a sustainable and eco-friendly alternative to petroleum-based plastics for fresh produce packaging.

Received 21st September 2025
Accepted 20th November 2025

DOI: 10.1039/d5fb00606f

rsc.li/susfoodtech

Sustainability spotlight

This study highlights the sustainability potential of chemically modified teff starch-based films as eco-friendly packaging alternatives to petroleum-based plastics. By improving mechanical strength, barrier properties, thermal stability, and UV protection, oxidized and cross-linked films effectively preserved the quality of fresh green grapes, reducing weight loss and extending shelf life. These biodegradable films address the growing demand for renewable, non-toxic, and compostable packaging materials, contributing to reduced plastic waste and environmental pollution. Their ability to enhance food preservation while minimizing reliance on synthetic polymers demonstrates a sustainable solution that aligns with circular economy principles and supports global efforts toward greener food systems.

1. Introduction

The packaging industry faces a key challenge in developing innovative materials to replace synthetic polymers. There is growing interest in finding biodegradable alternatives to traditional petroleum-based plastics. Due to its non-toxic nature, safety, abundance, renewability, and environmental friendliness, starch is widely recognized as one of the most promising raw materials for biodegradable plastic production.[1] However, its practical application is limited by its high hydrophilicity and brittleness. Starch can be modified through physical, chemical, enzymatic, or combined approaches to address these limitations to enhance its properties. Starch films have been primarily used in food packaging, where extended food shelf life requires films with high optical transparency, mechanical strength, and barrier properties. Numerous studies have indicated that the key technical challenge for starch films lies in enhancing their mechanical properties while minimizing water vapor permeability.[2] Teff starch, derived from the ancient grain teff (*Eragrostis tef*), has been increasingly recognized for its pivotal role in creating environmentally friendly, biodegradable materials. As global awareness of plastic pollution grows, the need for

Department of Food Engineering and Technology, Sant Longowal Institute of Engineering and Technology, Longowal, Punjab, India. E-mail: rmnsidhu1795@gmail.com

sustainable alternatives is becoming more urgent. This has led to a strong drive to develop biodegradable films that replace conventional synthetic plastics, especially in packaging applications. Developing such films is crucial in reducing the environmental impact of plastic waste. Teff starch's attractiveness lies in its biodegradability, renewability, and functional properties.[3]

Chemical modifications play a crucial role in improving starch functionality. Among these, starch oxidation, a chemical modification that employs an oxidizing agent in the starch at specific pH and temperature conditions, is another area of significant research. Oxidised starch with low viscosity, low retrogradation, high transparency, and high film forming is widely used in food, paper, and other industries.[4] The most used oxidants in the industry include sodium hypochlorite, potassium permanganate, hydrogen peroxide, *etc.* During oxidation, hydroxyl groups on the starch chains are converted into carbonyl and carboxyl groups, accompanied by partial cleavage of glycosidic linkages. These structural alterations enhance film formation and modify the physicochemical behavior of the starch.[5]

Moreover, crosslinking—a promising and cutting-edge technique—is crucial for enhancing the performance and applicability of polysaccharide-based films, particularly by reducing their water sensitivity.[6] Cross-linking agents, including citric acid (CA), sodium citrate (SC), and choline dihydrogen citrate salt, can enhance the tensile strength and thermal stability of starch films while reducing their solubility in water.[7] Numerous studies have been conducted on using citric acid to enhance polysaccharide-based films' physical and barrier properties.[8,9] Plasticizers are essential additives used in both natural and synthetic polymers to improve their flexibility and reduce brittleness. An ideal plasticiser should reduce intermolecular forces and moisture absorption, increase the mobility of starch chains, and be compatible with the biopolymer. Commonly used starch plasticisers are small molecules with polar functional groups, such as hydroxyl (–OH), carboxyl (–COOH), and amino ($–NH_2$) groups.[10]

Extensive research on oxidized and cross-linked starch biofilms derived from sources such as potato, cassava, and sorghum has unequivocally demonstrated significant improvements in mechanical strength and barrier properties.[11–13] However, despite these promising advancements, a critical research gap persists regarding the chemical modification of Indian teff starch—an underexplored yet highly promising raw material—and its potential for biodegradable film development. Addressing this gap is vital to harnessing teff starch as a sustainable and effective alternative for eco-friendly packaging solutions. To address this, the present study systematically investigated the effects of oxidation and cross-linking on Indian teff starch, focusing on key properties including mechanical strength, structural integrity, thermal stability, water vapor permeability, and biodegradability. Furthermore, the practical application of the modified teff starch films was evaluated by using them to package fresh grapes, thereby assessing the shelf life of the grapes. These findings not only provide critical insights into the functional performance of chemically modified teff starch but also underscore its potential as a sustainable, bio-based alternative to synthetic plastic films for active food packaging applications, particularly for perishable fruits.

2. Material and method

2.1. Materials

Teff grains were procured from the Kadamba Foundation, Bengaluru. All the chemicals used were analytical grade. Sodium hypochlorite was used as an oxidising agent, and citric acid was used as a cross-linker. The used chemicals were analytical grade and purchased from HiMedia BioSci, plot no. C40, road no. 21Y, MIDC, Wagle Industrial Estate, Thane (West)—400604, Maharashtra, India.

2.2. Starch isolation and modification

The teff starch was extracted following the method established in a previous study.[3] A modified procedure based on Zhou *et al.* (2016)[14] was used to oxidize teff starch. A 40% starch slurry was prepared by mixing 100 g of starch (dry basis) with deionized water to reach 250 g. The slurry was kept at 35 °C, and its pH was adjusted to 9.5 using 2 N NaOH. Sodium hypochlorite (NaOCl) was added gradually, with continuous stirring, at concentrations of 0.8 and 1.2 g of active chlorine per 100 g of starch, maintaining the pH at 9.5. After adding NaOCl, the slurry was held for 50 min, keeping the pH steady at 9.5 with 1 N NaOH. The mixture was then neutralized to pH 7.0 using 1 N H_2SO_4, filtered, rinsed with distilled water, and dried in an oven at 40 °C for 24 hours. The dried starch was ground and stored for further analysis.

Teff starch was cross-linked using citric acid following the method of Kim *et al.* (2017).[15] Citric acid, at levels of 10% and 20% based on starch weight, was dissolved in distilled water, and the solution's pH was adjusted to 3.5 using 10 M NaOH. This solution was then combined with 100 g of starch and incubated at 30 °C for 16 h. The mixture was centrifuged at 5000 rpm for 5 min and washed thrice to remove unreacted citric acid. The starch was then dried in an oven at 40 °C for 24 h, ground, and stored at 4 °C for future analysis.

2.3. Biofilm formation

Starch biofilms were prepared using the casting method, based on the procedure described by da Rosa Zavareze *et al.* (2012),[16] with minor modifications. A 3% starch solution was gelatinized at 90 °C for 30 min with continuous stirring. After cooling, 30% (v/w of starch) glycerol was added as a plasticiser, and the mixture was stirred at 150 rpm for 20 min. The solution was then cast onto a Teflon-coated baking tray. The cast films were dried in an oven at 50 °C for 16 hours. Once dried and cooled, the films were peeled off and conditioned at 25 °C for 48 hours before further analysis. The resulted starch films included native teff starch film (NF), oxidised films (O1F (0.8 g active chlorine), O2F (1.2 g active chlorine)), and cross-linked films (C1F (10% CA, C2F (20% CA))).

2.4. Characterisation of biofilms

2.4.1. Thickness, solubility, and moisture content of biofilms

2.4.1.1. Thickness. The digital display Vernier caliper was used to determine the thickness of biofilms with an accuracy of ±1 μm at different locations. The average was taken as follows:

$$\text{Thickness} = \frac{\text{sum of measured values}}{10} \quad (1)$$

2.4.1.2. Solubility. The solubility of films was determined according to the method by Colivet & Carvalho, 2017.[12] The dried film samples were immersed in 50 ml distilled water and kept in a shaking water bath at 25 °C for 24 h. The films were again dried for 24 h till constant weight was achieved. The solubility was calculated as:

$$\text{Solubility}(\%) = \frac{(m_1 - m_2)}{m_1} \times 100 \quad (2)$$

2.4.1.3. Moisture content. Film pieces (50 mm × 50 mm) were prepared and weighed (W_1), then dried at 105 °C for 24 h and weighed again (W_2). The moisture content was calculated as follows:

$$\text{Moisture content} = \frac{W_1 - W_2}{W_1} \times 100 \quad (3)$$

2.4.2. Barrier properties of water vapour and oxygen. The Water Vapor Permeability (WVP) of biofilms was calculated by the method of Fan *et al.* (2016)[17] with slight modifications. Hygroscopic $CaCl_2$ was added to about 3/4 of the conical flask, and the film was sealed over the top. The pre-weighed conical flask with a lid was kept at 38 °C and 90% relative humidity in an open desiccator. The weight gain of the film samples was measured at set intervals. The increase in weight due to moisture absorption by the $CaCl_2$ indicates the transmission of water vapor through the film. The average WVP was determined using the following equation:

$$\text{WVP} = \frac{\Delta m \times d}{t \times A \times \Delta p} \quad (4)$$

where Δm denotes the weight increase of the tube (g), d denotes film thickness, A area (m^2), t time for permeation (h), Δp partial water vapour pressure difference across the film (Pa).

Oxygen permeability in starch films was assessed by measuring the peroxide value. Approximately 10 ml of vegetable oil was placed in a conical flask tightly covered with starch films. After 20 days, the films were removed, and the oil's peroxide value was evaluated. The peroxide value was measured using the Yan *et al.* (2012)[18] method with some modifications. A 5 ml sample was taken, and 30 ml of acetic acid chloroform was added before heating the mixture. Then, 0.5 ml of potassium iodide solution was added and stirred thoroughly. Afterwards, 30 ml of distilled water was added, and the mixture was vigorously shaken. The sample was titrated using 0.1 N sodium thiosulphate from a burette, with 0.5 ml of starch as the indicator. The peroxide values were calculated using the formula:

$$\text{PV}\ (\text{mEq kg}^{-1}) = \frac{(S - B)\ \text{normality of sodium thiosulphate}}{\text{weight of sample}} \times 100 \quad (5)$$

where S and B are the titre volume of the sample and blank.

2.4.3. Contact angle. Contact angle measurements were carried out using the sessile drop method. A 3 μl droplet of deionised water was placed on the surface of the samples, and images were captured with a video camera at 0, 45, and 90 s after the droplet was applied. These images were used to analyse the interaction of water with the specimens over time, and the contact angle was measured using Matlab software.[19]

2.4.4. Mechanical properties. The mechanical properties were measured using a texture analyser (Stable Microsystems, Surrey, UK) to measure tensile strength (TS), elongation at break (EAB), and Young's modulus (YM) following the ASTME 96 standard[20] standard. The samples were cut into 1 × 7 cm. The initial separation distance was 100 mm, and the test speed was 1.0 mm s^{-1}.

2.4.5. UV protection of biofilms. The transparency of the film samples was assessed by measuring their percent transmittance across a wavelength range of 200 to 800 nm using a UV-visible spectrophotometer (Model UV5704SS). Data for transmittance within the UVA (315–400 nm) and UVB (280–315 nm) ranges were collected. The following equations were used for calculations:

$$\text{UVA} = \frac{T315 + T320 + T325 + \cdots + T395 + T400}{18} \quad (6)$$

$$\text{UVB} = \frac{T280 + T285 + T290 + T300 + T305 + T310 + T315}{8} \quad (7)$$

2.4.6. Thermogravimetric analysis (TGA). The thermal stability of films was assessed using a thermogravimetric analyser (TG 209 F1 Libra, NETZSCH-Gerätebau GmbH, Germany). Approximately 10 mg of films were put in an aluminium pan, and an empty aluminium container was used as a reference. The samples were heated from 30 to 600 °C at a rate of 10 °C min^{-1} in a nitrogen atmosphere, and the change in mass of the samples was measured.

2.4.7. Fourier transform infrared spectroscopy (FTIR). The FTIR was conducted using Perkin Elmer-Spectrum RX-1 FTIR, USA. The spectrum was recorded as transmittance across a wavelength of 4000 to 400 cm^{-1}.

2.4.8. X-ray diffraction (XRD). XRD of native and modified films was evaluated using an X-ray diffractometer (D8 ADVANCE, Bruker, Germany). The samples were scanned in a range of 5–80° of 2θ with a scanning speed of 2° min^{-1}. The total area under the curve and the area under each prominent peak were determined using the Origin Pro software, and per cent crystallinity was calculated using the formula below:

$$\text{Crystallinity } (\%) = \frac{\text{area under peaks}}{\text{total area}} \times 100 \quad (8)$$

2.4.9. Scanning electron microscopy (SEM). The microstructure of films was examined using SEM (SM 6610-LV, JEOL, Japan) at an accelerating voltage of 5 kV. The films were mounted on aluminium stubs using carbon adhesive tape on both sides and coated with a thin layer of gold before imaging at 2000 and 3000×.

2.4.10. Biodegradability in soil. The films were cut into 20 × 20 cm initially weighted and then placed in containers containing garden soil (pH 7 and moisture content 15%). The containers were kept at room temperature and covered with aluminum foil. The water was sprayed regularly to maintain the moisture. Samples were taken out after 5 days, and weight loss was checked. Percent weight loss was determined as a function of number of days:

$$\%\ \text{Weight loss} = \frac{\text{initial weight at begining} - \text{final weight after particular duration}}{\text{initial weight}} \times 100 \quad (9)$$

2.5.1. Application of native and chemically modified biofilms as green grapes packaging. Green grapes that were fresh, healthy, and free of physical damage or microbiological contamination were carefully chosen and sorted to guarantee consistency in ripeness, size, and color. After that, the selected grape samples were weighed and packaged using biofilms: NF, O1F, O2F, C1F, C2F and LDPE (Fig. 6). After that, packed grapes, were kept at 5 °C for 0, 2, 4, 6, 8 and 12 days to conduct additional analysis.

2.5.1.1. Weight loss. Weight loss was measured using a balance after 2, 4, 6, 8, 10, and 12 days of storage, and a decrease in weight was observed during this period.

2.5.1.2. pH. The pH of the green grape juice was measured using a Thermo Scientific™ Orion Star™ A214 pH/ISE Benchtop Meter. At each storage interval (2, 4, 6, 8, 10, and 12 days), 10 g of grapes were juiced from each packaging type. The juice was then diluted with distilled water to a final volume of 50 ml. The pH was determined by immersing the electrode in the juice solution and recording the value once the meter reading stabilised.[21]

2.5.1.3. Total soluble solids (TSS) and titratable acidity. Biochemical analyses of green grapes were conducted to determine their titratable acidity and total soluble solids (TSS). A hand-held refractometer (Erma, Japan) was used to determine the total soluble solids (TSS) at a temperature of 25 ± 1 °C, with the results expressed in degrees Brix (°Brix). Grape juice samples (10 ml) were diluted with 90 ml of distilled water, and a 10 ml aliquot of this mixture was titrated with standardised 0.1 N sodium hydroxide. The titration was carried out in the presence of phenolphthalein as an indicator, with the endpoint marked by the appearance of a persistent pink colour lasting at least fifteen seconds. To determine the titratable acidity (TA %) of the juice, the volume of sodium hydroxide used was converted to grams of citric acid per 100 ml of juice using the following equation.[22]

$$\text{TA } (\%) = \frac{T \times N \times V_1 \times E}{V \times V_2 \times 1000} \times 100 \quad (10)$$

where T is the titre volume (ml), N is the normality of standard NaOH, V_1 is the volume made up (ml), E is the equivalent weight of acid, V_2 is the aliquot volume (ml), and V is the volume of sample taken (ml).

2.5.1.4. Firmness. The compression test was conducted using a texture analyser (TA-XT2i, Stable Micro Systems, UK), calibrated with a 5 kg load cell. A cylindrical probe (P/5, 5 mm diameter) was operated at a speed of 5 mm s^{-1} to assess the hardness of green grapes. Samples were taken at various storage intervals from different packaging types, and the hardness values were recorded as force in Newtons (N).

2.6. Statistical analysis

The data were displayed as average values ± standard deviation. The analysis of variance (ANOVA) method was used with the SPSS 22.0 statistical analysis system to assess the difference between the factors and levels. The means were compared using Duncan's multiple range tests ($p < 0.05$).

3. Results and discussion

3.1. Thickness, solubility and moisture content

The thickness, solubility, and moisture content of films are shown in Table 1. Film thickness is a critical factor influencing its barrier properties and water vapor permeability. The thickness of the films ranged from 0.14 to 0.17 mm. OF exhibited the most significant thickness among the other biofilms can be attributed to carboxyl and carbonyl groups, which enhanced interactions with glycerol and promoted water retention during the film drying. This suggests that O2F has higher opacity and tensile strength. However, a less significant difference was seen in CF, but are less thick than OF because cross-linking agents interact with the hydroxyl groups in starch, forming di-ester linkages with the available OH groups. This process enhances the structural integrity of the films, resulting in less flexible, more rigid, and thicker films.[23]

Food packaging materials must be waterproof to prevent food spoilage. Therefore, biofilms should maintain a moisture content that benefits the packaging material. Reducing the moisture content of the material is one key area for enhancing biofilm production. The moisture content is reduced for O1F and O2F (8.23 and 7.34%), while NF (10.34%). The reduction in moisture content may be attributed to the carbonyl functional

Table 1 Thickness, solubility, moisture, water vapor permeability (WVP) and POV (oxygen permeation) of native and chemically modified teff starch biofilms[a]

Films	Thickness (mm)	Solubility (%)	Moisture (%)	WVP (10^{-8} g m^2 s Pa)	POV (g/100g)
NF	0.14 ± 0.01^{d}	30.34 ± 0.03^{a}	10.34 ± 0.15^{a}	4.09 ± 0.01^{a}	18.33 ± 0.20^{a}
O1F	0.16 ± 0.10^{b}	28.60 ± 0.03^{b}	8.23 ± 0.02^{d}	2.09 ± 0.03^{d}	10.55 ± 0.50^{e}
O2F	0.17 ± 0.11^{a}	21.76 ± 0.19^{d}	7.34 ± 0.13^{e}	2.52 ± 0.02^{c}	11.27 ± 0.41^{d}
C1F	0.15 ± 0.10^{c}	23.83 ± 0.02^{c}	8.63 ± 0.09^{c}	3.00 ± 0.03^{b}	15.98 ± 0.72^{b}
C2F	0.14 ± 0.12^{d}	20.70 ± 0.01^{e}	9.68 ± 0.17^{b}	3.98 ± 0.03 ^{ab}	12.18 ± 0.0^{c}

[a] Values are expressed as mean ± standard deviation. Different letters in the same column indicate significant differences among film samples ($p < 0.05$), NF = native film, O1F and O2F = oxidised films and CIF and C2F = cross-linked films.

groups in the oxidised starch, which exhibit hydrophobic characteristics. This hydrophobicity reduces the bonded and free water within the film, indirectly contributing to the decrease in moisture content. The C1F and C2F exhibited low moisture content (8.63 and 9.68%) due to crosslinkers resistance to water absorption.

Solubility reflects a film's integrity in aqueous environments, with high solubility indicating low resistance to water dissolution and low solubility signifying higher resistance. The decreased solubility of O1F and O2F (28.60 and 21.76%) was due to the added oxidized starch, which dispersed within the starch matrix and blocked the pores that would have allowed water penetration.[24] The solubility of C1F and C2F (23.83 and 20.70%) was also improved compared to NF (30.34%). This could be attributed to the reduced availability of hydrophilic hydroxyl groups and the formation of hydrophobic ester linkages between citric acid and polysaccharides, leading to a denser matrix and enhanced water insolubility. A similar changing pattern for improved solubility has been reported in cross-linked Litchi kernel starch.[25]

3.2. Water vapour permeability and oxygen permeability

Water vapour permeability (WVP) is a critical factor in biofilms, as it is a crucial indicator of how well the packaging can manage moisture exchange between the food and its environment. The WVP is valuable in determining the effectiveness of a specific film in preventing or allowing moisture exchange. The O1F and O2F showed 38–49% decreased WVP than NF as the introduced carbonyl groups exhibited a lower affinity for water molecules than the hydroxyl groups in starch, resulting in a reduced capacity of the biofilm to facilitate water transfer. A similar decrease in WVP was observed in oxidized mango kernel starch films.[26] The slight decrease in WVP of C1F and C2F is attributed to reinforcement that restricts water vapor transmission by limiting the movement of starch chains in the amorphous regions.[27] Additionally, reducing WVP values may be linked to substituting hydrophilic hydroxyl groups with hydrophobic ester groups in the polymer. On the other hand, the more robust interactions between crosslinked starch and other film-forming components. This may have resulted in a denser biofilm structure, limiting water vapour transmission.[28] These findings indicated that O1F and O2F had the potential for use in food packaging, as they exhibit reduced permeability and lower water migration through the film, which are crucial for adequate food packaging.

The oxygen barrier properties of packaging materials were essential for maintaining food quality by preventing oxygen from penetrating. Oxygen can trigger oxidation, cause spoilage, and support the growth of aerobic microorganisms.[29] The POV of the native and modified films were presented in Table 1.

The POV of the biofilms ranges from 10.55 to 18.33 g/100 g. Starch-based films typically exhibit excellent oxygen barrier properties due to forming a tightly packed, ordered matrix held together by hydrogen bonds. Additionally, their hydrophilic nature reduces interactions with oxygen molecules, which are inherently hydrophobic.[30] The O1F and O2F and C1F and C2F showed an improved oxygen barrier compared to NF, possibly due to the incorporation of carboxyl or hydroxyl groups, which further decreased the oxygen barrier.[31] The key reason is the hydrogen bonding between the amylose molecules in starch and the added functional groups. These hydrogen bonds create a more compact, tightly packed network within the films. This denser molecular arrangement constricts the pathways through which gas molecules can diffuse, effectively reducing gas permeability. The more restricted the movement of gas molecules, the less permeable the film becomes, further enhancing its function as a barrier against oxygen.[11,32]

3.3. Water contact angle (WCA)

The water contact angle measures how liquid interacts with a solid surface, indicating the hydrophilicity and hydrophobicity of the surface. Generally, the surfaces with $\theta > 65°$ are hydrophobic, while those with $\theta < 65°$ are hydrophilic. The WCA of the native and modified starch biofilms are shown in Table 2. The WCA of NF is 51.32° and increased for O1F and O2F at 58.81° and 60.17°, respectively. The introduction of carboxyl and carbonyl groups through oxidation effectively limits water interaction by reducing the number of free hydroxyl groups, thereby making the starch surface more hydrophobic and increasing the contact angle. The WCA was also increased for C1F and C2F (63.35° and 62.26°). This may be attributed to the formation of hydrophobic ester bonds between citric acid and the polysaccharides, reduced the number of polar groups and consequently limiting water absorption on the film's surface.[33] Additionally, it has been reported that rough surfaces can exhibit significantly larger contact angles due to heterogeneous wetting. Other researchers have also observed similar changes

Table 2 The contact angle of native and modified teff starch biofilms

Biofilms	Angle (°)	Image
NF	51.32	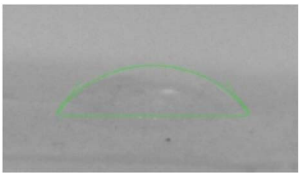
OF1	58.81	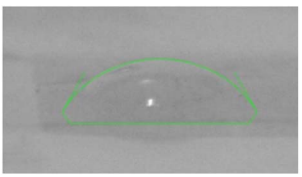
OF2	60.17	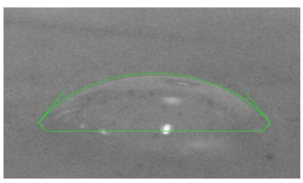
CF1	63.35	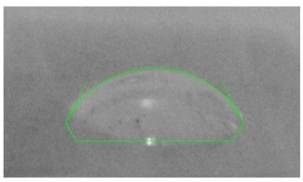
CF2	62.26	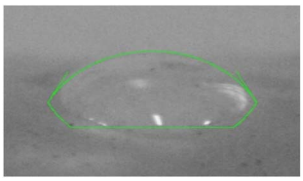

in water contact angle for polysaccharide-based films incorporating tea polyphenols and cassava starch films.[16,34]

3.4. Mechanical properties

The mechanical properties of starch-based biofilms, such as tensile strength (TS), elongation at break (EAB), and Young's Modulus (YM), are crucial in determining the material's ability to endure external stresses while preserving its structural integrity without tearing. These characteristics are essential in defining the appropriate film applications and the handling guidelines for products packaged with these materials.[35]

Oxidised films showed an approximately two-fold increase in TS, attributed to the introduction of carbonyl and carboxyl groups that promoted stronger intermolecular interactions and a denser polymer network (Table 3). An increased amount of oxidized starch results in higher tensile strength, possibly because the greater presence of oxidized starch enhances polymer chain interactions, leading to a more compact film structure that requires greater force to break. The increase in TS was also reported in oxidised Lotus Rhizome and Sorghum starch films.[36,37]

EAB provides insight into the stretchability and flexibility of biofilms. The EAB of NF (38.21%) was significantly increased for O1F and O2F. Intermolecular interactions occur between the hydroxyl groups of starch and the carbonyl groups of oxidised starch, potentially leading to an extended chain length in the biofilm molecules. This chain extension might have enhanced the biofilm's extensibility, resulting in greater EAB.[38] The higher the YM, the higher the stiffness of biofilms. The OF showed greater YM (3.72 and 3.91 MPa).

The TS also showed comparable increase in C1F and C2F as the amount of cross linker increased, TS also increased and decreased EAB but further increasing cross linker concentration decreaser the TS. Citric acid can function as both a crosslinking agent and a plasticizer in biopolymer films, particularly at higher concentrations. The excess unreacted citric acid likely behaves as a plasticizer, weakening the interactions between macromolecules, which leads to a reduction in TS and an increase in EAB. Cross-linked starch molecules strengthen intermolecular interactions, including covalent and hydrogen bonds, which enhance the mechanical properties of the film.[39] The EAB of C1F and C2F decreased (2–3% lower) because cross-linked starch possesses a stronger structure compared to native starch, owing to the presence of diphosphate linkages. These linkages restrict the mobility of cross-linked starch chains, resulting in a reduction in the EAB value. Cross-linking generally increases the YM of biofilms. This is because the formation of covalent bonds (such as diphosphate linkages) between starch molecules enhances the stiffness of the film's structure. It can be concluded that using CA within an optimal range as

Table 3 Tensile strength (TS), Young's modulus (YM), elongation at break (EAB), UVA, UVB, and transparency of native and chemically modified teff starch biofilms[a]

Films	TS (MPa)	YM (MPa)	EAB (%)	UVA	UVB	Transparency (%)	DO (1047/1016)	DD (995/722)	DD (1730/1711)
NF	3.07 ± 0.11^{d}	2.27 ± 0.10^{e}	38.21 ± 0.21^{e}	18.18	6.8	48.85	1.19 ± 0.02^{c}	0.94 ± 0.10^{e}	1.01 ± 0.03^{b}
O1F	7.88 ± 0.21^{a}	3.72 ± 0.18^{b}	39.57 ± 0.17^{b}	13.55	3.75	43.69	1.22 ± 0.03^{a}	0.98 ± 0.02^{b}	1.00 ± 0.01^{c}
O2F	7.90 ± 0.32^{a}	3.91 ± 0.12^{a}	39.74 ± 0.25^{a}	16.95	5.45	46.39	1.20 ± 0.02^{b}	0.10 ± 0.12^{a}	1.02 ± 0.10^{a}
C1F	6.62 ± 0.23^{c}	2.82 ± 0.21^{d}	37.52 ± 0.16^{c}	9.73	1.81	31.19	1.18 ± 0.04^{d}	0.95 ± 0.03^{d}	1.02 ± 0.02^{a}
C2F	6.71 ± 0.34^{b}	3.02 ± 0.15^{c}	37.79 ± 0.13^{d}	13.53	4.08	46.39	1.17 ± 0.03^{e}	0.97 ± 0.02^{c}	1.01 ± 0.12^{b}

[a] Values are expressed as mean ± standard deviation. Different letters in the same column indicate ± significant differences among film samples ($p < 0.05$), NF = native film, O1F and O2F = oxidised films and CIF and C2F = cross-linked films.

a crosslinking agent can effectively modify the properties of biofilms. However, when used in excess, CA behaves as a plasticizer, negatively affecting the film's characteristic.

3.5. UV-visible spectra analysis of biofilms

Ultraviolet light transmission is critical in designing packaging to ensure product protection and preservation until it reaches consumers. Although only 3% of the sun's total radiation is ultraviolet, it is sufficient to trigger chemical reactions and degrade packaging materials. UV radiation spans wavelengths from 100 to 400 nm, with UVC (100–280 nm) entirely absorbed by the ozone layer. However, UVA (315–400 nm) and UVB (280–315 nm) still reach the Earth's surface and can affect packaging materials.[40,41]

The UV transmission spectra of each biofilm and transmittance values were shown in Table 3. The figure showed that NF had higher transparency (48.85%) and transmitted 18% UVA with 6.8% UVB (Table 3). Hence, NF offered less protection against UVA and UVB, making it unsuitable for applications with strong UV blocking. On the other hand, O1F and O2F showed 43.69% and 46.39% transparency with UVA (13.55%, 16.95%) and UVB (3.75%, 5.45%), which allowed a moderate level of UV protection. The C1F and C2F had transparency 31.19% and 46.39%, UVA (9.73% and 13.53%), and UVB (1.81% and 4.08%). C1F and C2F exhibited lower transmittance in UVA and UVB, possibly due to their denser, more complex structures, which scatter or absorb UVA and UVB light more effectively. According to this study, C1F would be more effective in protecting against UVA and UVB.

3.6. TGA

The thermal stability of native and modified starch biofilms was explored using thermogravimetric analysis to analyze the structural interaction between polymers. Fig. 1 illustrates the thermal degradation of NF, OF, and CF as a function of temperature. The TGA curve revealed two stages of thermal degradation (Fig. 1). In the initial stage (approximately 30 °C to 150 °C), all film samples showed thermal stability up to 150 °C with weight loss up to 3 to 7%. The weight loss is likely due to the evaporation of water that is either weakly physically or firmly chemically bound within all the samples.[42] NF loses around 5% of its weight, O1F around 6%, O2F about 7%, C1F around 4%, and C2F only 3%, indicating its low moisture or volatile content. The primary thermal degradation process occurs in the second stage, where significant weight losses are observed. In this stage, the degradation of all samples takes place within a temperature range of approximately 150 °C to 400 °C. This stage also marks the point where the primary weight loss can be identified. O2F experiences the most significant degradation at 43%, suggesting lower thermal stability, followed by O1F at 41%, NF at 37%, and C2F at 35%. C2F shows the least degradation at 34%, highlighting its resilience to thermal breakdown. This degradation zone is linked to the breakdown of carbonaceous material. Wang *et al.* (2019)[43] suggested that the gradual thermal degradation in this area results from the continued carbonization and the cleavage of C–H and C–C bonds in the polysaccharide chains. Among all samples, C2F emerges as the most thermally stable, with the lowest weight loss across both stages. This suggests that cross-linking in C2F enhances its resistance to high temperatures and makes it the most suitable choice for applications requiring greater thermal stability.

3.7. FTIR

FTIR analysis was performed to identify the potential functional chemical groups and molecular interactions in the biofilms. The regions from 3000 to 3800 cm^{-1}, 2800 to 3000 cm^{-1}, and 1680 to 1760 cm^{-1} are associated with the stretching vibrations of O–H, C–H, and C–O bonds, respectively. Additionally, the polymer fingerprint region exhibited absorption within the range of 500 to 1500 cm^{-1}.[44,45] The prominent peaks at 1016 cm^{-1} and 1047 cm^{-1} are attributed to the C–O–H bending vibration and the C–O groups within anhydroglucose rings,

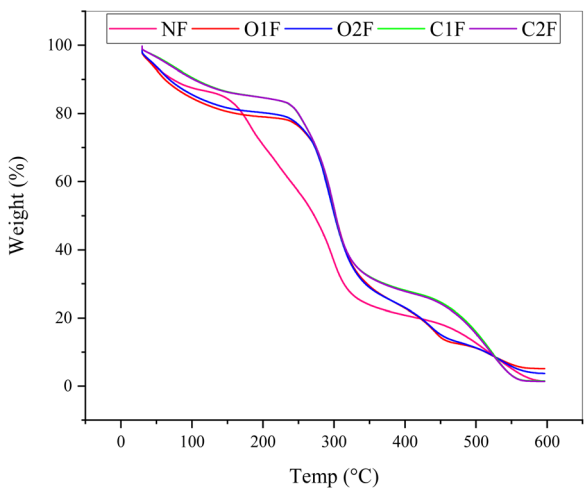

Fig. 1 TGA of native and modified teff starch biofilms, NF = native film, O1F and O2F = oxidised films and C1F and C2F = cross-linked films.

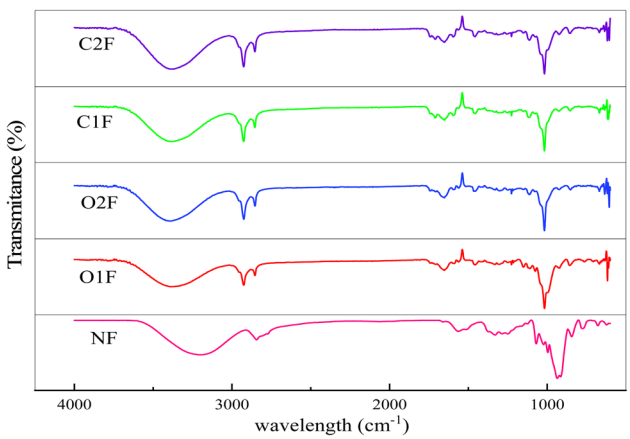

Fig. 2 FTIR spectra of native and modified teff starch biofilms, NF = native, O1F and O2F = oxidised films and C1F and C2F = cross-linked films.

which are sensitive to disordered amorphous and ordered crystalline starch structures.[46] The intensity ratios between the peaks at 1047 cm^{-1} and 1016 cm^{-1} (I_{1047}/I_{1016}) represent the relative proportion of the crystalline to amorphous regions. The (I_{1047}/I_{1016}) values indicated that the crystalline fraction followed the order O1F > O2F > NF > C1F, and C2F showed minimal impact on the crystalline fraction within the starch phase (Table 2).

Additionally, the peak at 995 cm^{-1} is primarily associated with C–O–H bending vibrations and is influenced by intramolecular hydrogen bonding of the –OH groups.[8] The (I_{995}/I_{727}) indicated that the matrices had an affinity for water through H-bonding and was increased in OF and CF, suggesting the more ordered arrangement within the material (O2F > O1F > CIF > C2F > NF). New peaks appeared in 1728, 1752, 1263, and 1760 cm^{-1} in OF and CF (Fig. 2). The intensity ratios between the peaks at 1730 cm^{-1} and 1711 cm^{-1} (I_{1730}/I_{1711}) reflected the crystalline fraction in the biofilms.[47] All the biofilms exhibited identical I_{1730}/I_{1711} values, indicating minimal impact on the molecular organization of biofilms. These peaks resulted from structural modifications that indicate interactions between the modified starches and the film-forming components. In the modified starch films, the 1728, 1752, and 1760 cm^{-1} peaks are associated with carboxyl groups and carboxylic esters. The peaks at 1263 and 1271 cm^{-1}, observed in the spectra of oxidized and cross-linked biofilms, correspond to phosphate stretching (P–O–C and P═O) vibrations.

3.8. XRD

X-ray diffraction (XRD) analysis was used to examine the effect of oxidizing and crosslinking agents on the crystalline structure of the biofilms.[48] The native and modified starch biofilms displayed a semicrystalline structure, evident from a sharp crystalline peak and a broad, amorphous hump in the diffraction pattern with a predominantly amorphous region, typical of thermally processed starch materials (Fig. 3). The diffraction patterns for biofilms showed peaks at specific 2θ angles: a very small peak at 15.21°, a narrow peak at 17.09°, a broad small peak at 18.21°, and a small peak at 23.04°. This can be attributed to minor alterations in the starch crystal structure for OF, as oxidation primarily affects the amorphous region. The key difference noted was an increase in crystallinity in the O1F and O2F (15.55 and 15.91%) compared to NF (13.37%), with crystallinity rising alongside higher oxidation levels. The partial cleavage of glycosidic bonds during oxidation likely promoted the recrystallization of amylose and amylopectin during film drying, resulting in more crystalline material formation.[49] The crystallinity of C1F and C2F (12.17 and 12.47%) was observed to

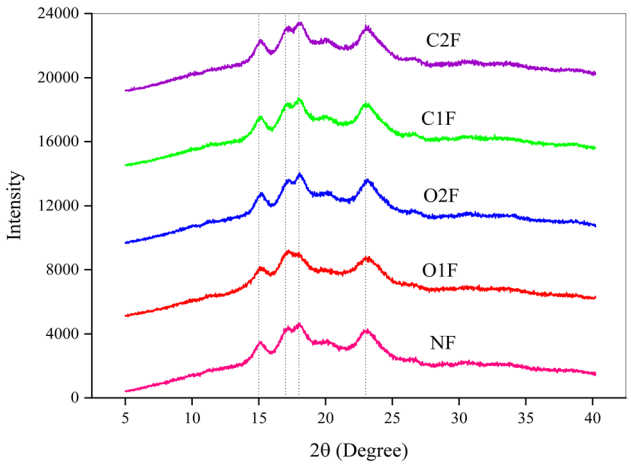

Fig. 3 XRD patterns of native and modified teff starch biofilms.

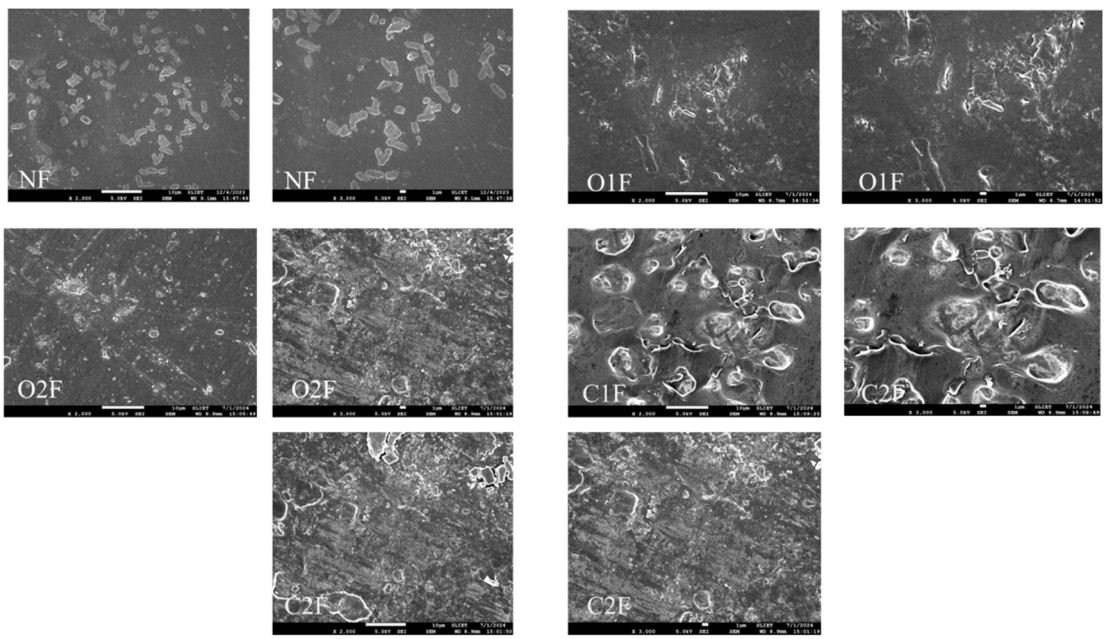

Fig. 4 SEM images of native and modified teff starch biofilms, NF = native, O1F and O2F = oxidised films and CIF and C2F = cross-linked films.

be lower than that of NF, with further reduction as the level of modification increased. The bulky, hydrophilic phosphate groups hindered the aggregation of leached amylose chains, limiting the formation of junction zones and thereby reducing the crystallinity of the crosslinked starch films. This reduction in crystallinity might result from reorientation in some regions during the drying process.[41]

3.9. Scanning electron microscopy (SEM)

The effects of oxidation and cross-linking on the morphology of biofilms were evaluated using Scanning Electron Microscopy (SEM). It was observed from Fig. 4 that O1F and O2F showed more homogeneous and uniform surfaces than NF, which showed the presence of starch granules. The uniformity of biofilms was attributed to the depolymerization of starch during oxidation, which facilitated greater penetration of the plasticizer chains and enhanced interactions between the components responsible for film formation.[12] Further, C1F showed some visible texture on the surface with starch granules, possibly due to a low cross-linker concentration. However, C2F showed a smooth, compact, and uniform surface indicating high degree of cross linking. This improvement can be attributed to the esterification reaction between the carboxyl groups of citric acid and the hydroxyl groups of starch, forming intermolecular ester linkages that reinforced the polymer network and reduced surface irregularities. This resulted in greater intermolecular connections by increasing the degree of cross-linking inside the starch matrix. Glycerol and carboxymethyl cellulose (CMC) were more compatible with the modified starches, which led to improved structural cohesion and homogeneous polymer blending. The enhanced interfacial bonding of the modified films was confirmed to have contributed to their greater tensile strength and structural integrity by the good correlation between these morphological features

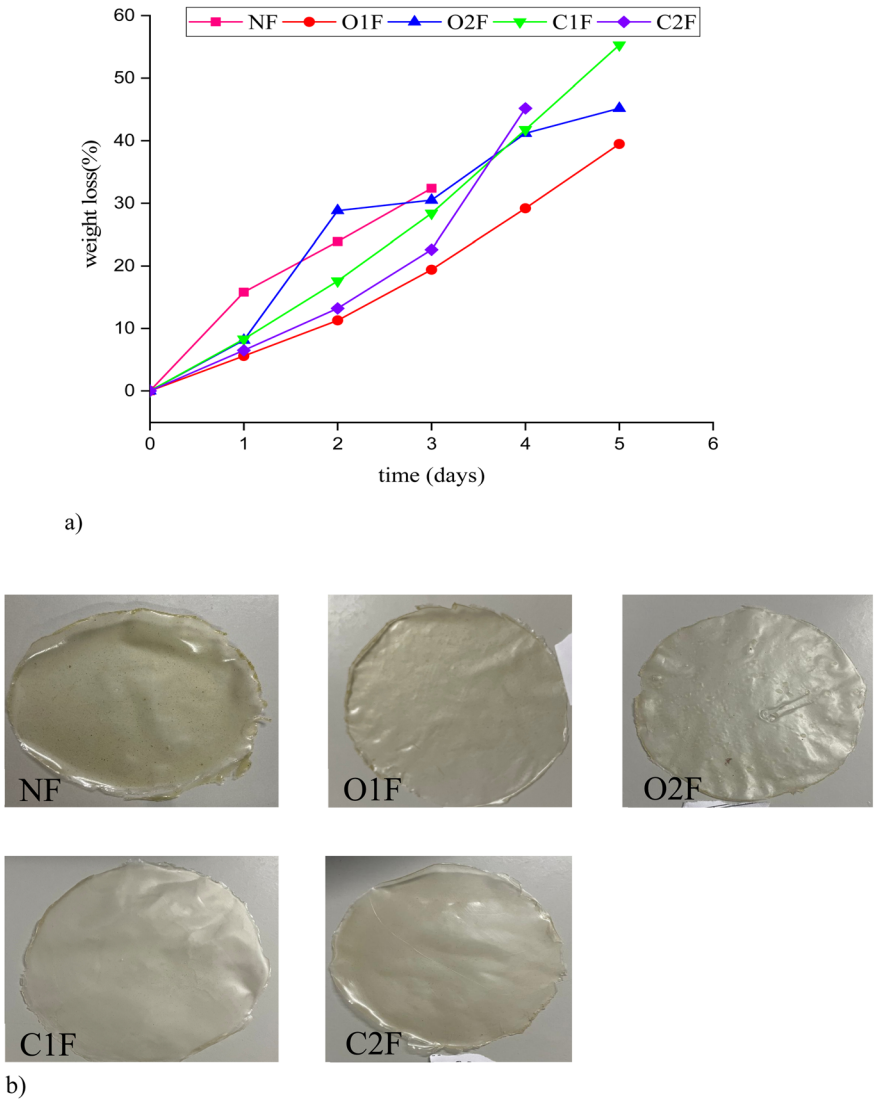

Fig. 5 (a) Biodegradability of native and modified teff starch biofilms. (b) Biofilms NF = native, O1F and O2F = oxidised films and CIF and C2F = cross-linked films.

shown in SEM images and their improved mechanical properties.

3.10. Biodegradability

The biodegradability of the teff starch biofilms was evaluated under soil burial conditions. Biodegradation involves the breakdown of physico-mechanical properties, material fragmentation, and chemical changes driven by enzymes and microorganisms. The biodegradability of bioplastics can be influenced by factors such as the microbial environment, soil moisture, weather conditions, and biofilm characteristics like moisture content, density, and the presence of plant bioactive, which can either enhance or hinder the degradation process.[50]

Fig. 5a depicted the weight loss percent of biofilms over a 5 day storage period under soil. All samples exhibited a consistent increase in weight loss over time, indicating progressive moisture loss during soil burial. Among the treatments, O1F showed the lowest weight loss, reaching approximately 35% by day 5, suggesting it had the most effective moisture barrier properties. In contrast, C1F and C2F demonstrated the highest weight loss, with values around 55% and 45%, respectively, indicating a weaker capacity to prevent dehydration. The NF and O2F films showed intermediate performance, with weight loss ranging

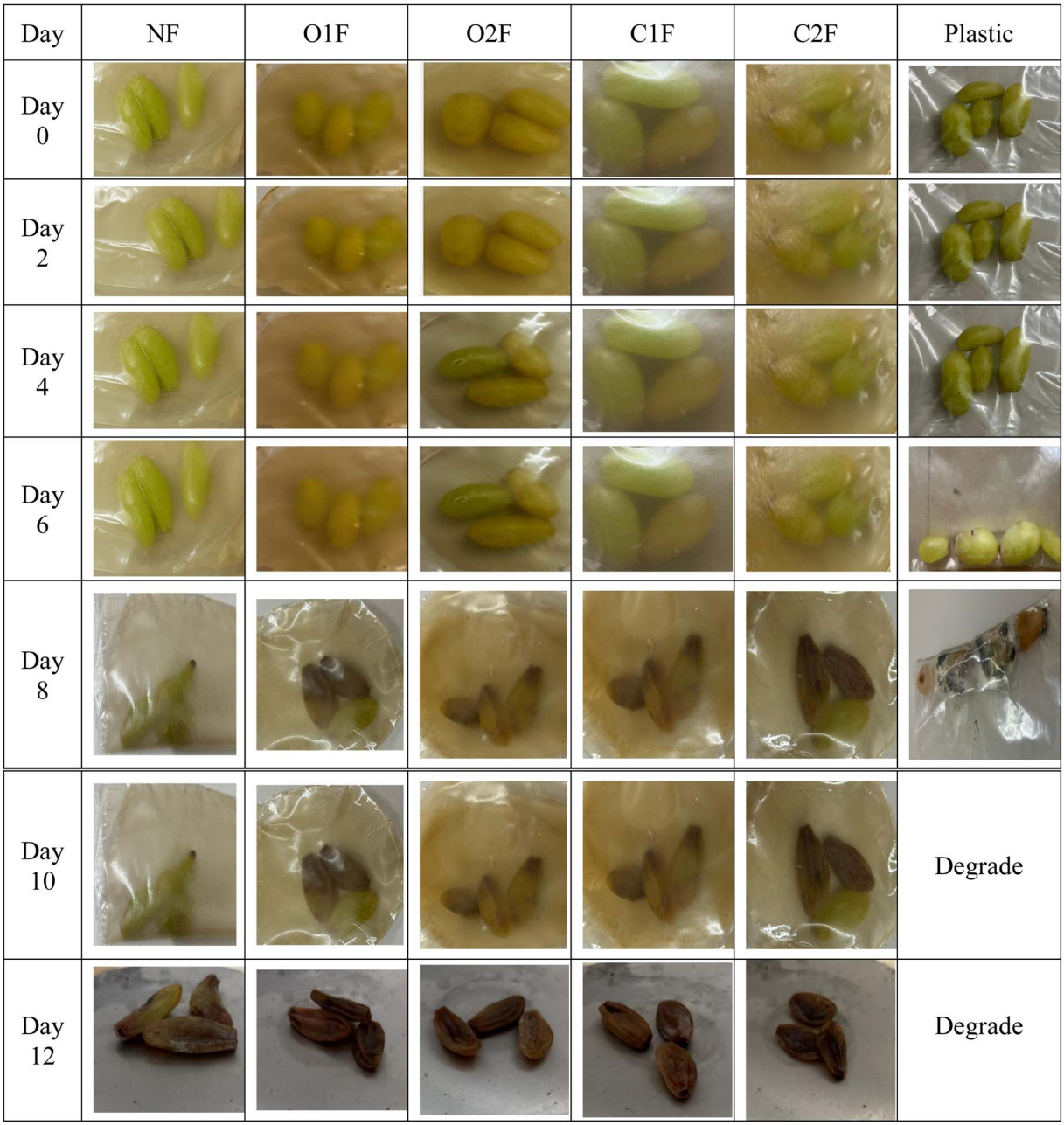

Fig. 6 Green grapes stored at 5 °C for 0, 2, 4, 6, 8, 10, and 12 days with N – native film, O1F, O2F – oxidised films, C1F, C2F – cross linked films and plastic.

between 40 and 45% at the end of the storage period. These results confirmed that oxidized starch-based films, particularly O1F, were more efficient in reducing water vapor permeability and preserving the freshness of grapes, aligning with previously reported WVP data.

3.11. Characterisation of green grapes

3.11.1. Storage and weight loss. The preservation capability of food packaging films was a key factor influencing their practical application, and visual appearance serves as the most direct indicator for assessing quality. As illustrated in Fig. 6, the appearance of grapes during storage was monitored and photographed. By day 6, noticeable differences in the visual condition of grapes were observed depending on the type of packaging. In the LDPE, significant wrinkling and decay occurred, primarily due to moisture loss and exposure to oxygen. As storage time progressed, the air-exposed grapes exhibited even more severe shrinkage and rotting.

The teff starch biofilms improved preservation compared to the plastic packaging. Grapes wrapped in native and modified teff starch biofilms maintained their integrity for up to 8 days, but by day 10, signs of shrivelling and wrinkling became evident. Weight loss in grapes primarily resulted from respiration and transpiration, driven by the water vapour pressure gradient between the fruit and its surrounding environment.

Table 4 Characterisation of green grapes packed in native and modified biofilms from 0 to 12 days[a]

	NF	O1F	O2F	C1F	C2F	Plastic
Weight						
Day 0	7.91 ± 0.09^{a}	7.46 ± 0.08^{a}	7.92 ± 0.80^{a}	7.38 ± 0.65^{a}	6.57 ± 0.09^{a}	8.03 ± 0.05^{a}
Day 2	7.80 ± 0.10^{b}	7.37 ± 0.06^{b}	7.80 ± 0.10^{b}	7.30 ± 0.51^{b}	6.48 ± 0.11^{b}	7.93 ± 0.09^{b}
Day 4	7.71 ± 0.08^{c}	7.26 ± 0.05^{c}	7.73 ± 0.10^{c}	7.23 ± 0.07^{c}	6.39 ± 0.11^{c}	7.83 ± 0.11^{c}
Day 6	7.63 ± 0.04^{d}	7.16 ± 0.04^{d}	7.62 ± 0.12^{d}	7.11 ± 0.07^{d}	6.30 ± 0.01^{d}	7.74 ± 0.08^{d}
Day 8	7.55 ± 0.05^{e}	7.04 ± 0.06^{e}	7.54 ± 0.10^{e}	7.00 ± 0.07^{e}	6.21 ± 0.02^{e}	7.64 ± 0.09^{d}
Day 10	7.53 ± 0.02^{e}	7.00 ± 0.04^{e}	7.50 ± 0.02^{f}	6.94 ± 0.04^{f}	6.17 ± 0.01^{e}	ND
Day 12	ND	ND	ND	ND	ND	ND
pH						
Day 0	3.66 ± 0.01^{c}	3.71 ± 0.03^{e}	3.62 ± 0.02^{e}	3.70 ± 0.03^{e}	3.61 ± 0.01^{e}	3.62 ± 0.02^{e}
Day 2	3.68 ± 0.04^{c}	3.76 ± 0.01^{d}	3.78 ± 0.04^{d}	3.76 ± 0.05^{d}	3.73 ± 0.05^{d}	3.70 ± 0.01^{d}
Day 4	3.84 ± 0.08^{c}	3.90 ± 0.01^{c}	3.91 ± 0.07^{c}	3.91 ± 0.02^{c}	3.85 ± 0.04^{c}	3.86 ± 0.10^{c}
Day 6	3.91 ± 0.07^{b}	3.98 ± 0.02^{b}	3.99 ± 0.06^{b}	3.99 ± 0.02b	3.92 ± 0.03^{b}	3.93 ± 0.02^{b}
Day 8	4.88 ± 0.06^{a}	5.21 ± 0.09^{a}	4.79 ± 0.08^{a}	5.30 ± 0.08^{a}	5.06 ± 0.07^{a}	4.63 ± 0.05^{a}
Day 10	ND	ND	ND	ND	ND	ND
Day 12	ND	ND	ND	ND	ND	ND
TSS						
Day 0	14.90 ± 0.09^{c}	15.21 ± 0.07^{b}	15.21 ± 0.07^{c}	15.34 ± 0.04^{b}	15.46 ± 0.01^{d}	15.44 ± 0.01^{e}
Day 2	14.81 ± 0.06^{a}	15.03 ± 0.06^{a}	14.80 ± 0.06^{a}	15.14 ± 0.04^{a}	15.11 ± 0.07^{a}	15.16 ± 0.04^{a}
Day 4	14.74 ± 0.04^{b}	14.91 ± 0.02^{c}	14.71 ± 0.03^{b}	15.00 ± 0.01^{b}	14.99 ± 0.02^{b}	14.83 ± 0.03^{b}
Day 6	14.43 ± 0.03^{d}	14.63 ± 0.03^{d}	14.58 ± 0.07^{d}	14.68 ± 0.04^{c}	14.79 ± 00.06^{c}	14.47 ± 0.04^{c}
Day 8	14.23 ± 0.02^{e}	14.35 ± 0.07^{e}	14.32 ± 0.04^{e}	14.40 ± 0.06^{d}	14.42 ± 0.02^{e}	14.38 ± 0.06^{d}
Day 10	ND	ND	ND	ND	ND	ND
Day 12	ND	ND	ND	ND	ND	ND
Acidity						
Day 0	0.35 ± 0.05^{c}	0.54 ± 0.05^{d}	0.59 ± 0.06^{a}	0.67 ± 0.08^{a}	0.46 ± 0.07^{a}	0.48 ± 0.06^{a}
Day 2	0.30 ± 0.01^{a}	0.50 ± 0.04^{a}	0.48 ± 0.03^{b}	0.53 ± 0.03^{b}	0.41 ± 0.04^{b}	0.30 ± 0.05^{b}
Day 4	0.24 ± 0.01^{a}	0.44 ± 0.03^{b}	0.34 ± 0.04^{b}	0.51 ± 0.02^{b}	0.38 ± 0.03^{c}	0.26 ± 0.04^{c}
Day 6	0.19 ± 0.02^{b}	0.38 ± 0.04^{b}	0.30 ± 0.04^{c}	0.47 ± 0.01^{c}	0.35 ± 0.04^{d}	0.24 ± 0.05^{c}
Day 8	0.17 ± 0.02^{b}	0.30 ± 0.04^{c}	0.24 ± 0.03^{c}	0.44 ± 0.01^{c}	0.33 ± 0.03^{d}	0.21 ± 0.05^{c}
Day 10	ND	ND	ND	ND	ND	ND
Day 12	ND	ND	ND	ND	ND	ND
Firmness						
Day 0	12.71 ± 0.07^{d}	12.73 ± 0.07^{b}	12.93 ± 0.06^{a}	12.58 ± 0.08^{a}	12.31 ± 0.05^{c}	13.06 ± 0.06^{a}
Day 2	12.99 ± 0.04^{a}	12.83 ± 0.05^{a}	12.67 ± 0.04^{b}	12.58 ± 0.07^{a}	12.48 ± 0.06^{a}	12.92 ± 0.04^{b}
Day 4	12.89 ± 0.02^{b}	12.71 ± 0.01^{b}	12.57 ± 0.06^{c}	12.50 ± 0.06^{b}	12.39 ± 0.05^{b}	12.84 ± 0.05^{c}
Day 6	12.79 ± 0.04^{c}	12.59 ± 0.04^{c}	12.46 ± 0.08^{d}	12.42 ± 0.07^{c}	12.29 ± 0.04^{d}	12.76 ± 0.06^{d}
Day 8	12.69 ± 0.06^{e}	12.48 ± 0.04^{d}	12.37 ± 0.04^{e}	12.33 ± 0.09^{d}	12.20 ± 0.08^{e}	12.71 ± 0.07^{e}
Day 10	ND	ND	ND	ND	ND	ND
Day 12	ND	ND	ND	ND	ND	ND

[a] Values are expressed as mean ± standard deviation. Different letters in the same column indicate significant differences among film samples ($p < 0.05$).

When weight loss exceeds 5%, it typically diminishes the market value of fruits and vegetables. As shown in Table 4, green grapes progressively lost weight during storage, with plastic-packed grapes experiencing the most rapid decline. By the 10th day, grapes stored in LDPE were no longer monitored due to significant quality deterioration, rendering them inedible. Notably, the use of native and modified teff starch biofilms significantly slowed the rate of weight loss over time. These films effectively preserved the grapes' freshness for a longer period and were more efficient in extending their shelf life. This enhanced performance can be attributed to the uniform distribution of the rigid, crystalline nature of biofilms, which likely created a tortuous path that impeded gas and vapour exchange.[51] Hence, the weight loss investigation showed that teff starch-based biofilms can be used as a packaging material for green grapes. Furthermore, the strong water vapour barrier properties of the teff starch biofilms contributed to reduced water loss.

3.11.2. Titratable acidity, pH and total soluble solids (TSS). Organic acids play a key role in shaping the overall flavour profile of grape berries. The acidity in grapes primarily results from the accumulation of citric acid as the fruit ripens. However, once grapes reach full ripeness, citric acid levels begin to decline.[52] During fruit development, total acidity rises, peaking at the green (unripe) stage, and then gradually decreases as the fruit overripenes. Titratable acidity is influenced not only by the type of packaging but also by storage temperature. As indicated in Table 4, pH values increase while titratable acidity decreases over the storage period. This reduction in acidity is a clear indicator of the fruit's progression toward maturation. Similar results were observed by Ghosh *et al.* (2020)[53] in storage studies of grapes using a biodegradable film from banana pseudostem.

The total soluble solids (TSS) of green grapes stored for 10 days using different packaging materials. The TSS values declined from 14.90 to 14.42 °Brix for both native and modified teff starch biofilms, and from 15.44 to 14.38 °Brix for LDPE, respectively, by the eighth day of storage. This reduction in TSS may be attributed to an increased respiration rate, which activates metabolic enzymes. Similar findings were reported by Joo *et al.* (2011) and Bangar *et al.* (2022),[54,55] where blackberries stored in bio-based packaging at low temperatures exhibited minimal to no changes in TSS, and red grapes stored in starch-based films reinforced with cellulosic nanocrystals and essential oil exhibited a decrease in TSS.

3.11.3. Firmness. Fruit firmness is a vital quality characteristic closely linked to consumer preference, as firmer fruits are typically perceived as juicier, crispier, and more appealing. Loss of firmness can also be associated with weight reduction and damage caused by microbial spoilage or decay. The grape firmness declined noticeably over the storage period, as shown in Table 4, which correlates with the loss of moisture over time. Firmness dropped from 12.71 to 12.69 N, 12.73 TO 12.37 N for O1F and O2F, 12.93 to 12.33 N for C1F and C2F and 13.06 to 12.71 N for LDPE by the tenth day.

The least reduction in firmness occurred in grapes packaged with modified biofilms, indicating that this film composition was most effective in preserving fruit texture. Additionally, incorporating a pickering emulsion likely enhanced the cross-linking of starch chains and reduced chain mobility by occupying voids in the matrix.[1] This restricted water permeability helped retain the fruit's moisture and firmness during storage.

4. Conclusion

This study showed that the physicochemical and functional characteristics of the resultant films were greatly enhanced by the chemical modification of teff starch through oxidation and cross-linking. In comparison to native starch films, the modified films demonstrated improved mechanical strength, superior barrier performance, and increased thermal stability. However, the film from the cross-linked starch showed a decreased water vapor permeability. Besides the films from oxidized starch demonstrated enhanced transparency and moderate flexibility. Therefore, chemically modified biofilms demonstrated improved UV protection, reducing the transmission of damaging radiation a crucial feature for extending the shelf life of packaged goods. Additionally, the developed films demonstrated practical usefulness in perishable fruit preservation when applied to green grape packaging, as weight loss was effectively reduced, acidity decline was delayed, and fruit firmness was maintained during storage.

These results demonstrate that chemical modification can significantly improve the performance of teff starch films, making them sustainable substitutes for polymers derived from petroleum. Further investigation is required to assess industrial-scale production, long-term biodegradation behavior, and economic viability to ascertain their commercial potential in sustainable packaging applications.

Author contributions

Ramandeep Kaur Sidhu: writing – original draft, investigation, formal analysis, conceptualization. C. S. Riar: writing – review & editing, validation. Sukhcharn Singh: writing – review & editing, validation, supervision.

Conflicts of interest

There is no conflict of interest.

Data availability

Data will be made available on request to the authors.

References

1 S. P. Bangar, W. S. Whiteside, A. Chowdhury, R. A. Ilyas and A. K. Siroha, Recent advancements in functionality, properties, and applications of starch modification with stearic acid: A review, *Int. J. Biol. Macromol.*, 2024, **280**, 135782.
2 B. C. Maniglia, N. Castanha, P. Le-Bail, A. Le-Bail and P. E. Augusto, Starch modification through

environmentally friendly alternatives: A review, *Crit. Rev. Food Sci. Nutr.*, 2021, **61**(15), 2482–2505.
3 R. K. Sidhu, C. S. Riar and S. Singh, Influence of heat moisture, ultrasonication, and gamma irradiation on pasting, thermal, morphological, and physicochemical properties of Indian teff (*Eragrostis tef*) starch, *Starch-Stärke*, 2024, e2300241.
4 N. L. Vanier, S. L. M. El Halal, A. R. G. Dias and E. da Rosa Zavareze, Molecular structure, functionality and applications of oxidized starches: A review, *Food Chem.*, 2017, **221**, 1546–1559.
5 B. Biduski, F. T. da Silva, W. M. da Silva, S. L. D. M. El Halal, V. Z. Pinto, A. R. G. Dias and E. da Rosa Zavareze, Impact of acid and oxidative modifications, single or dual, of sorghum starch on biodegradable films, *Food Chem.*, 2017, **214**, 53–60.
6 F. Garavand, M. Rouhi, S. H. Razavi, I. Cacciotti and R. Mohammadi, Improving the integrity of natural biopolymer films used in food packaging by crosslinking approach: A review, *Int. J. Biol. Macromol.*, 2017, **104**, 687–707.
7 M. Escamilla-Garcia, A. Reyes-Basurto, B. E. Garcia-Almendarez, E. Hernández-Hernández, G. Calderón-Domínguez, G. Rossi-Marquez and C. Regalado-Gonzalez, Modified starch–chitosan edible films: Physicochemical and mechanical characterization, *Coatings*, 2017, **7**(12), 224.
8 P. G. Seligra, C. M. Jaramillo, L. Famá and S. Goyanes, Biodegradable and non-retrogradable eco-films based on starch–glycerol with citric acid as crosslinking agent, *Carbohydr. Polym.*, 2016, **138**, 66–74.
9 R. Priyadarshi, B. Kumar and Y. S. Negi, Chitosan film incorporated with citric acid and glycerol as an active packaging material for extension of green chilli shelf life, *Carbohydr. Polym.*, 2018, **195**, 329–338.
10 G. A. Duarte, M. C. Bezerra, S. H. Bettini and A. A. Lucas, Real-time monitoring of the starch cross-linking with citric acid by chemorheological analysis, *Carbohydr. Polym.*, 2023, **311**, 120733.
11 L. M. Fonseca, J. R. Gonçalves, S. L. M. El Halal, V. Z. Pinto, A. R. G. Dias, A. C. Jacques and E. da Rosa Zavareze, Oxidation of potato starch with different sodium hypochlorite concentrations and its effect on biodegradable films, *LWT–Food Sci. Technol.*, 2015, **60**(2), 714–720.
12 J. Colivet and R. A. Carvalho, Hydrophilicity and physicochemical properties of chemically modified cassava starch films, *Ind. Crops Prod.*, 2017, **95**, 599–607.
13 S. Mehboob, T. M. Ali, M. Sheikh and A. Hasnain, Effects of cross-linking and/or acetylation on sorghum starch and film characteristics, *Int. J. Biol. Macromol.*, 2020, **155**, 786–794.
14 F. Zhou, Q. Liu, H. Zhang, Q. Chen and B. Kong, Potato starch oxidation induced by sodium hypochlorite and its effect on functional properties and digestibility, *Int. J. Biol. Macromol.*, 2016, **84**, 410–417.
15 J. Y. Kim, Y. K. Lee and Y. H. Chang, Structure and digestibility properties of resistant rice starch cross-linked with citric acid, *Int. J. Food Prop.*, 2017, **20**(sup2), 2166–2177.
16 E. da Rosa Zavareze, V. Z. Pinto, B. Klein, S. L. M. El Halal, M. C. Elias, C. Prentice-Hernández and A. R. G. Dias, Development of oxidised and heat-moisture treated potato starch film, *Food Chem.*, 2012, **132**(1), 344–350.
17 H. Fan, N. Ji, M. Zhao, L. Xiong and Q. Sun, Characterization of starch films impregnated with starch nanoparticles prepared by 2,2,6,6-tetramethylpiperidine-1-oxyl (TEMPO)-mediated oxidation, *Food Chem.*, 2016, **192**, 865–872.
18 Q. Yan, H. Hou, P. Guo and H. Dong, Effects of extrusion and glycerol content on properties of oxidized and acetylated corn starch-based films, *Carbohydr. Polym.*, 2012, **87**(1), 707–712.
19 E. Ojogbo, R. Blanchard and T. Mekonnen, Hydrophobic and melt processable starch–laurate esters: Synthesis, structure–property correlations, *J. Polym. Sci., Part A:Polym. Chem.*, 2018, **56**(23), 2611–2622.
20 ASTM E96, *Standard Test Methods for Water Vapor Transmission of Materials*, ASTM International, West Conshohocken, PA, 1996.
21 S. L. M. El Halal, R. Colussi, V. Z. Pinto, J. Bartz, M. Radunz, N. L. V. Carreño and E. da Rosa Zavareze, Structure, morphology and functionality of acetylated and oxidised barley starches, *Food Chem.*, 2015, **168**, 247–256.
22 S. M. Hosseini, B. Hosseinzadeh Samani, S. Rostami and Z. Lorigooini, Design and characterisation of jet cold atmospheric pressure plasma and its effect on *Escherichia coli*, colour, pH, and bioactive compounds of sour cherry juice, *Int. J. Food Sci. Technol.*, 2021, **56**(10), 4883–4892.
23 Y. Tanetrungroj and J. Prachayawarakorn, Effect of dual modification on properties of biodegradable crosslinked-oxidized starch and oxidized-crosslinked starch films, *Int. J. Biol. Macromol.*, 2018, **120**, 1240–1246.
24 J. Prachayawarakorn and P. Kansanthia, Characterization and properties of singly and dually modified hydrogen peroxide oxidized and glutaraldehyde crosslinked biodegradable starch films, *Int. J. Biol. Macromol.*, 2022, **194**, 331–337.
25 V. Sharma, M. Kaur, K. S. Sandhu, V. Nain and S. Janghu, Physicochemical and rheological properties of cross-linked litchi kernel starch and its application in development of bio-films, *Starch-Stärke*, 2021, **73**(7–8), 2100049.
26 A. J. Vellaisamy Singaram, S. Guruchandran, A. Bakshi, C. Muninathan and N. D. Ganesan, Study on enhanced mechanical, barrier and optical properties of chemically modified mango kernel starch films, *Packag. Technol. Sci.*, 2021, **34**(8), 485–495.
27 G. A. Gebresas, T. Szabó and K. Marossy, A comparative study of carboxylic acids on the cross-linking potential of corn starch films, *J. Mol. Struct.*, 2023, **1277**, 134886.
28 B. S. Kalsi, S. Singh, M. S. Alam and S. Bhatia, Application of thermosonication for guava juice processing: Impacts on bioactive, microbial, enzymatic and quality attributes, *Ultrason. Sonochem.*, 2023, **99**, 106595.
29 S. Galus and J. Kadzińska, Moisture sensitivity, optical, mechanical and structural properties of whey protein-based edible films incorporated with rapeseed oil, *Food Technol. Biotechnol.*, 2016, **54**(1), 78–89.

30 R. Kumar, K. Park, K. Ahn, J. R. Ansari, K. Sadeghi and J. Seo, Maleic acid crosslinked starch/polyvinyl alcohol blend films with improved barrier properties for packaging applications, *Int. J. Biol. Macromol.*, 2024, **271**, 132495.
31 K. Huntrakul, R. Yoksan, A. Sane and N. Harnkarnsujarit, Effects of pea protein on properties of cassava starch edible films produced by blown-film extrusion for oil packaging, *Food Packag. Shelf Life*, 2020, **24**, 100480.
32 M. Sapper, P. Talens and A. Chiralt, Improving functional properties of cassava starch-based films by incorporating xanthan, gellan, or pullulan gums, *Int. J. Polym. Sci.*, 2019, **2019**(1), 5367164.
33 M. Faisal, T. Kou, Y. Zhong and A. Blennow, High amylose-based bio composites: Structures, functions and applications, *Polymers*, 2022, **14**(6), 1235.
34 H. G. Song, I. Choi, J. S. Lee, M. N. Chung, C. S. Yoon and J. Han, Comparative study on physicochemical properties of starch films prepared from five sweet potato (*Ipomoea batatas*) cultivars, *Int. J. Biol. Macromol.*, 2021, **189**, 758–767.
35 J. Uranga, A. I. Puertas, A. Etxabide, M. T. Dueñas, P. Guerrero and K. De La Caba, Citric acid-incorporated fish gelatin/chitosan composite films, *Food Hydrocolloids*, 2019, **86**, 95–103.
36 S. Sukhija, S. Singh and C. S. Riar, Development and characterization of biodegradable films from whey protein concentrate, psyllium husk and oxidized, crosslinked, dual-modified lotus rhizome starch composite, *J. Sci. Food Agric.*, 2019, **99**(7), 3398–3409.
37 B. Biduski, F. T. da Silva, W. M. da Silva, S. L. D. M. El Halal, V. Z. Pinto, A. R. G. Dias and E. da Rosa Zavareze, Impact of acid and oxidative modifications, single or dual, of sorghum starch on biodegradable films, *Food Chem.*, 2017, **214**, 53–60.
38 H. Wu, Y. Lei, J. Lu, R. Zhu, D. Xiao, C. Jiao and M. Li, Effect of citric acid induced crosslinking on the structure and properties of potato starch/chitosan composite films, *Food Hydrocolloids*, 2019, **97**, 105208.
39 V. Sharma, M. Kaur, K. S. Sandhu and S. K. Godara, Effect of cross-linking on physico-chemical, thermal, pasting, *in vitro* digestibility and film forming properties of faba bean (*Vicia faba* L.) starch, *Int. J. Biol. Macromol.*, 2020, **159**, 243–249.
40 M. Shaikh, S. Haider, T. M. Ali and A. Hasnain, Physical, thermal, mechanical and barrier properties of pearl millet starch films as affected by levels of acetylation and hydroxypropylation, *Int. J. Biol. Macromol.*, 2019, **124**, 209–219.
41 Y. K. Dasan, A. H. Bhat and F. Ahmad, Polymer blend of PLA/PHBV based bionanocomposites reinforced with nanocrystalline cellulose for potential application as packaging material, *Carbohydr. Polym.*, 2017, **157**, 1323–1332.
42 B. González-Torres, M. A. Robles-García, M. Gutiérrez-Lomelí, J. J. Padilla-Frausto, C. L. Navarro-Villarruel, C. L. Del-Toro-Sánchez and F. J. Reynoso-Marín, Combination of sorbitol and glycerol, as plasticizers, and oxidized starch improves the physicochemical characteristics of films for food preservation, *Polymers*, 2021, **13**(19), 3356.
43 Z. Wang, Z. Yao, J. Zhou, M. He, Q. Jiang, A. Li and D. Zhang, Improvement of polylactic acid film properties through the addition of cellulose nanocrystals isolated from waste cotton cloth, *Int. J. Biol. Macromol.*, 2019, **129**, 878–886.
44 M. R. Area, B. Montero, M. Rico, L. Barral, R. Bouza and J. López, Properties and behavior under environmental factors of isosorbide-plasticized starch reinforced with microcrystalline cellulose biocomposites, *Int. J. Biol. Macromol.*, 2020, **164**, 2028–2037.
45 C. Zhang, Z. Wang, Y. Li, Y. Yang, X. Ju and R. He, The preparation and physiochemical characterization of rapeseed protein hydrolysate–chitosan composite films, *Food Chem.*, 2019, **272**, 694–701.
46 A. B. D. Nandiyanto, R. Ragadhita and M. Fiandini, Interpretation of Fourier transform infrared spectra (FTIR): A practical approach in the polymer/plastic thermal decomposition, *Indones. J. Sci. Technol.*, 2023, **8**(1), 113–126.
47 S. F. Yao, X. T. Chen and H. M. Ye, Investigation of structure and crystallization behavior of poly (butylene succinate) by fourier transform infrared spectroscopy, *J. Phys. Chem. B*, 2017, **121**(40), 9476–9485.
48 T. Woggum, P. Sirivongpaisal and T. Wittaya, Characteristics and properties of hydroxypropylated rice starch based biodegradable films, *Food Hydrocolloids*, 2015, **50**, 54–64.
49 A. O. Kalu, E. C. Egwim, A. A. Jigam and H. L. Muhammad, Effect of oxidized sucrose, citric acid crosslinking and dual modification on some physicochemical properties of cassava starch for potential application in packaging films, *BIOMED Nat. Appl. Sci.*, 2022, **2**(2), 10–24.
50 U. Shah, F. Naqash, A. Gani and F. A. Masoodi, Art and science behind modified starch edible films and coatings: a review, *Compr. Rev. Food Sci. Food Saf.*, 2016, **15**(3), 568–580.
51 G. Ghoshal and H. Chopra, Impact of apricot oil incorporation in tamarind starch/gelatin based edible coating on shelf life of grape fruit, *J. Food Meas. Charact.*, 2022, **16**(2), 1274–1290.
52 Y. F. Zeng, Y. Y. Chen, Y. Y. Deng, C. Zheng, C. Z. Hong, Q. M. Li and X. Q. Zha, Preparation and characterization of lotus root starch based bioactive edible film containing quercetin-encapsulated nanoparticle and its effect on grape preservation, *Carbohydr. Polym.*, 2024, **323**, 121389.
53 M. Ghosh and P. Ghosh, Storage study of grapes (*Vitis vinifera*) using the nanocomposite biodegradable film from banana pseudostem, *J. Food Process. Preserv.*, 2020, **44**(12), e14917.
54 S. P. Bangar, W. S. Whiteside, F. Ozogul, K. D. Dunno, G. A. Cavender and P. Dawson, Development of starch-based films reinforced with cellulosic nanocrystals and essential oil to extend the shelf life of red grapes, *Food Biosci*, 2022, **47**, 101621.
55 M. Joo, N. Lewandowski, R. Auras, J. Harte and E. Almenar, Comparative shelf life study of blackberry fruit in bio-based and petroleum-based containers under retail storage conditions, *Food Chem.*, 2011, **126**(4), 1734–1740.